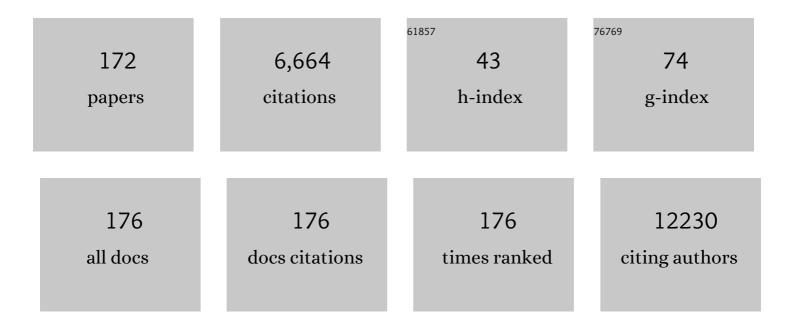
List of Publications by Year in descending order

Source: https://exaly.com/author-pdf/3288536/publications.pdf Version: 2024-02-01



**SHOTA ΝΑΚΑΜΠΡΑ** 

#	Article	IF	CITATIONS
1	Dysbiosis Contributes to Arthritis Development via Activation of Autoreactive T Cells in the Intestine. Arthritis and Rheumatology, 2016, 68, 2646-2661.	2.9	463
2	The Lipid Mediator Protectin D1 Inhibits Influenza Virus Replication and Improves Severe Influenza. Cell, 2013, 153, 112-125.	13.5	399
3	Oral pathobiont induces systemic inflammation and metabolic changes associated with alteration of gut microbiota. Scientific Reports, 2014, 4, 4828.	1.6	384
4	Guidance of regulatory T cell development by Satb1-dependent super-enhancer establishment. Nature Immunology, 2017, 18, 173-183.	7.0	300
5	Direct Metagenomic Detection of Viral Pathogens in Nasal and Fecal Specimens Using an Unbiased High-Throughput Sequencing Approach. PLoS ONE, 2009, 4, e4219.	1.1	240
6	Metagenomic Analysis Reveals Dynamic Changes of Whole Gut Microbiota in the Acute Phase of Intensive Care Unit Patients. Digestive Diseases and Sciences, 2016, 61, 1628-1634.	1.1	173
7	Plasmodium cynomolgi genome sequences provide insight into Plasmodium vivax and the monkey malaria clade. Nature Genetics, 2012, 44, 1051-1055.	9.4	172
8	Lypd8 promotes the segregation of flagellated microbiota and colonic epithelia. Nature, 2016, 532, 117-121.	13.7	167
9	Gut Microbiota of Healthy and Malnourished Children in Bangladesh. Frontiers in Microbiology, 2011, 2, 228.	1.5	157
10	Generation of colonic IgA-secreting cells in the caecal patch. Nature Communications, 2014, 5, 3704.	5.8	121
11	Metagenomic profile of gut microbiota in children during cholera and recovery. Gut Pathogens, 2013, 5, 1.	1.6	118
12	Metagenomic Diagnosis of Bacterial Infections. Emerging Infectious Diseases, 2008, 14, 1784-1786.	2.0	116
13	Metagenomic Analysis of Healthy and White Plague-Affected Mussismilia braziliensis Corals. Microbial Ecology, 2013, 65, 1076-1086.	1.4	103
14	Metagenomic analysis of DNA viruses in a wastewater treatment plant in tropical climate. Environmental Microbiology, 2012, 14, 441-452.	1.8	98
15	Performance comparison of second- and third-generation sequencers using a bacterial genome with two chromosomes. BMC Genomics, 2014, 15, 699.	1.2	93
16	Solution Structure of the Variable-Type Domain of the Receptor for Advanced Glycation End Products: New Insight into AGEâ^'RAGE Interaction <sup>,</sup> . Biochemistry, 2008, 47, 12299-12311.	1.2	90
17	Post-Golgi anterograde transport requires GARP-dependent endosome-to-TGN retrograde transport. Molecular Biology of the Cell, 2015, 26, 3071-3084.	0.9	88
18	Baseline Assessment of Mesophotic Reefs of the Vitória-Trindade Seamount Chain Based on Water Quality, Microbial Diversity, Benthic Cover and Fish Biomass Data. PLoS ONE, 2015, 10, e0130084.	1.1	81

#	Article	IF	CITATIONS
19	Fungal ITS1 Deep-Sequencing Strategies to Reconstruct the Composition of a 26-Species Community and Evaluation of the Gut Mycobiota of Healthy Japanese Individuals. Frontiers in Microbiology, 2017, 8, 238.	1.5	79
20	Giant Hall Resistivity and Magnetoresistance in Cubic Chiral Antiferromagnet EuPtSi. Journal of the Physical Society of Japan, 2018, 87, 023701.	0.7	79
21	Indigo Naturalis ameliorates murine dextran sodium sulfate-induced colitis via aryl hydrocarbon receptor activation. Journal of Gastroenterology, 2017, 52, 904-919.	2.3	78
22	Genetic characterization of blaNDM-harboring plasmids in carbapenem-resistant Escherichia coli from Myanmar. PLoS ONE, 2017, 12, e0184720.	1.1	74
23	Amphipathic α-Helices in Apolipoproteins Are Crucial to the Formation of Infectious Hepatitis C Virus Particles. PLoS Pathogens, 2014, 10, e1004534.	2.1	73
24	Genome-Wide Screening Uncovers the Significance of N-Sulfation of Heparan Sulfate as a Host Cell Factor for Chikungunya Virus Infection. Journal of Virology, 2017, 91, .	1.5	73
25	Genotypic Profile of <i>Streptococcus suis</i> Serotype 2 and Clinical Features of Infection in Humans, Thailand. Emerging Infectious Diseases, 2011, 17, 835-842.	2.0	70
26	Physiologic and metagenomic attributes of the rhodoliths forming the largest CaCO3 bed in the South Atlantic Ocean. ISME Journal, 2014, 8, 52-62.	4.4	68
27	BEC, a Novel Enterotoxin of Clostridium perfringens Found in Human Clinical Isolates from Acute Gastroenteritis Outbreaks. Infection and Immunity, 2014, 82, 2390-2399.	1.0	67
28	Plasmodium berghei ANKA causes intestinal malaria associated with dysbiosis. Scientific Reports, 2015, 5, 15699.	1.6	67
29	A Cluster of Fatal Tick-borne Encephalitis Virus Infection in Organ Transplant Setting. Journal of Infectious Diseases, 2017, 215, 896-901.	1.9	67
30	Effect of Hydration on the Stability of the Collagen-like Triple-Helical Structure of [4(R)-Hydroxyprolyl-4(R)-hydroxyprolylglycine]10‡. Biochemistry, 2005, 44, 15812-15822.	1.2	61
31	Fatal sepsis caused by an unusual Klebsiella species that was misidentified by an automated identification system. Journal of Medical Microbiology, 2013, 62, 801-803.	0.7	60
32	Electrostatically constrained α-helical peptide inhibits replication of HIV-1 resistant to enfuvirtide. International Journal of Biochemistry and Cell Biology, 2009, 41, 891-899.	1.2	59
33	Clonal dissemination of human isolates of Streptococcus suis serotype 14 in Thailand. Journal of Medical Microbiology, 2009, 58, 1508-1513.	0.7	58
34	GPAT2, a mitochondrial outer membrane protein, in piRNA biogenesis in germline stem cells. Rna, 2013, 19, 803-810.	1.6	56
35	Structural basis for PPARÎ <sup>3</sup> transactivation by endocrine-disrupting organotin compounds. Scientific Reports, 2015, 5, 8520.	1.6	56
36	Mutation accumulation under UV radiation in Escherichia coli. Scientific Reports, 2017, 7, 14531.	1.6	55

#	Article	IF	CITATIONS
37	Next-generation sequencing (NGS) in the identification of encephalitis-causing viruses: Unexpected detection of human herpesvirus 1 while searching for RNA pathogens. Journal of Virological Methods, 2015, 226, 1-6.	1.0	54
38	The presence of colistin resistance gene mcr-1 and -3 in ESBL producing Escherichia coli isolated from food in Ho Chi Minh City, Vietnam. FEMS Microbiology Letters, 2018, 365, .	0.7	52
39	<i>N</i> -Glycan–dependent protein folding and endoplasmic reticulum retention regulate GPI-anchor processing. Journal of Cell Biology, 2018, 217, 585-599.	2.3	51
40	Searching for Gap Zeros in Sr <sub>2</sub> RuO <sub>4</sub> via Field-Angle-Dependent Specific-Heat Measurement. Journal of the Physical Society of Japan, 2018, 87, 093703.	0.7	51
41	High salt intake increases plasma trimethylamine N-oxide (TMAO) concentration and produces gut dysbiosis in rats. Nutrition, 2018, 54, 33-39.	1.1	50
42	Sensitivity of Next-Generation Sequencing Metagenomic Analysis for Detection of RNA and DNA Viruses in Cerebrospinal Fluid: The Confounding Effect of Background Contamination. Advances in Experimental Medicine and Biology, 2016, , 53-62.	0.8	49
43	Molecular Characterization of IMP-1-Producing Enterobacter cloacae Complex Isolates in Tokyo. Antimicrobial Agents and Chemotherapy, 2018, 62, .	1.4	48
44	Temporal dynamics of bacterial microbiota in the human oral cavity determined using an in situ model of dental biofilms. Npj Biofilms and Microbiomes, 2016, 2, 16018.	2.9	47
45	CompleteÂThermal-UnfoldingÂProfilesÂofÂOxidizedÂandÂReducedÂCytochromesÂc. Journal of the American Chemical Society, 2004, 126, 14684-14685.	6.6	46
46	Hydrogen-Rich Saline Regulates Intestinal Barrier Dysfunction, Dysbiosis, and Bacterial Translocation in a Murine Model of Sepsis. Shock, 2018, 50, 640-647.	1.0	43
47	Non-Ischemic Heart Failure With Reduced Ejection Fraction Is Associated With Altered Intestinal Microbiota. Circulation Journal, 2018, 82, 1640-1650.	0.7	41
48	Allergic conversion of protective mucosal immunity against nasal bacteria in patients with chronic rhinosinusitis with nasal polyposis. Journal of Allergy and Clinical Immunology, 2019, 143, 1163-1175.e15.	1.5	39
49	Heme ameliorates dextran sodium sulfate-induced colitis through providing intestinal macrophages with noninflammatory profiles. Proceedings of the National Academy of Sciences of the United States of America, 2018, 115, 8418-8423.	3.3	38
50	Identification of a Golgi GPI-N-acetylgalactosamine transferase with tandem transmembrane regions in the catalytic domain. Nature Communications, 2018, 9, 405.	5.8	37
51	Two N-Linked Glycosylation Sites in the V2 and C2 Regions of Human Immunodeficiency Virus Type 1 CRF01_AE Envelope Glycoprotein gp120 Regulate Viral Neutralization Susceptibility to the Human Monoclonal Antibody Specific for the CD4 Binding Domain. Journal of Virology, 2010, 84, 4311-4320.	1.5	35
52	Prognostic Impact of Tumor Size Eliminating the Ground Glass Opacity Component: Modified Clinical T Descriptors of the Tumor, Node, Metastasis Classification of Lung Cancer. Journal of Thoracic Oncology, 2013, 8, 1551-1557.	0.5	35
53	Plasmid dynamics in Vibrio parahaemolyticus strains related to shrimp Acute Hepatopancreatic Necrosis Syndrome (AHPNS). Infection, Genetics and Evolution, 2017, 51, 211-218.	1.0	34
54	Five Amino Acid Residues Responsible for the High Stability of Hydrogenobacter thermophilus Cytochrome c552. Journal of Biological Chemistry, 2005, 280, 5527-5532.	1.6	33

#	Article	IF	CITATIONS
55	Structure and reaction mechanism of human nicotinamide phosphoribosyltransferase. Journal of Biochemistry, 2010, 147, 95-107.	0.9	33
56	Metagenomic analysis of bacterial infections by means of high-throughput DNA sequencing. Experimental Biology and Medicine, 2011, 236, 968-971.	1.1	31
57	Characterization of miR-122-independent propagation of HCV. PLoS Pathogens, 2017, 13, e1006374.	2.1	31
58	Regnase-1 controls colon epithelial regeneration via regulation of mTOR and purine metabolism. Proceedings of the National Academy of Sciences of the United States of America, 2018, 115, 11036-11041.	3.3	31
59	Phenotype-genotype correlations of PIGO deficiency with variable phenotypes from infantile lethality to mild learning difficulties. Human Mutation, 2017, 38, 805-815.	1.1	29
60	Gap structure of FeSe determined by angle-resolved specific heat measurements in applied rotating magnetic field. Physical Review B, 2017, 96, .	1.1	29
61	Virus purification and enrichment by hydroxyapatite chromatography on a chip. Sensors and Actuators B: Chemical, 2014, 201, 185-190.	4.0	27
62	Unique Electronic States in Non-centrosymmetric Cubic Compounds. Journal of Electronic Materials, 2017, 46, 3572-3584.	1.0	27
63	Detection of circulating Asian H5N1 viruses by a newly established monoclonal antibody. Biochemical and Biophysical Research Communications, 2009, 378, 197-202.	1.0	26
64	Roles of a short connecting disulfide bond in the stability and function of psychrophilic Shewanella violacea cytochrome c 5*. Extremophiles, 2007, 11, 797-807.	0.9	25
65	Comprehensive metagenomic approach for detecting causative microorganisms in culture-negative infective endocarditis. International Journal of Cardiology, 2014, 172, e288-e289.	0.8	25
66	Does ground glass opacity-dominant feature have a prognostic significance even in clinical T2aN0M0 lung adenocarcinoma?. Lung Cancer, 2015, 89, 38-42.	0.9	25
67	A novel <i>PIGN</i> mutation and prenatal diagnosis of inherited glycosylphosphatidylinositol deficiency. American Journal of Medical Genetics, Part A, 2016, 170, 183-188.	0.7	25
68	A comprehensive analysis of reassortment in influenza A virus. Biology Open, 2012, 1, 385-390.	0.6	24
69	The cell envelope–associated phospholipid-binding protein LmeA is required for mannan polymerization in mycobacteria. Journal of Biological Chemistry, 2017, 292, 17407-17417.	1.6	24
70	Clonal evolution and antigen recognition of anti-nuclear antibodies in acute systemic lupus erythematosus. Scientific Reports, 2017, 7, 16428.	1.6	24
71	Metagenomic Analysis of Cerebrospinal Fluid from Patients with Multiple Sclerosis. Advances in Experimental Medicine and Biology, 2016, 935, 89-98.	0.8	23
72	Structure of Cytochromec552 from a Moderate Thermophilic Bacterium,Hydrogenophilus thermoluteolus: Comparative Study on the Thermostability of Cytochromec‡. Biochemistry, 2006, 45, 6115-6123.	1.2	22

#	Article	IF	CITATIONS
73	Hyperstability and crystal structure of cytochrome <i>c</i> <sub>555</sub> from hyperthermophilic <i>Aquifex aeolicus</i> . Acta Crystallographica Section D: Biological Crystallography, 2009, 65, 804-813.	2.5	22
74	Rapid and simultaneous identification of three mutations by the Novaplexâ"¢ SARS-CoV-2 variants I assay kit. Journal of Clinical Virology, 2021, 141, 104877.	1.6	22
75	Assembly states of the nucleosome assembly protein 1 (NAP-1) revealed by sedimentation velocity and non-denaturing MS. Biochemical Journal, 2011, 436, 101-112.	1.7	21
76	Quasiparticle excitations and evidence for superconducting double transitions in monocrystalline U0.97Th0.03Be13. Physical Review B, 2017, 96, .	1.1	21
77	Fluctuation-Induced First-Order Transition and Tricritical Point in EuPtSi. Journal of the Physical Society of Japan, 2019, 88, 093701.	0.7	21
78	Genotypic Characterization of CRF01_AE <i>env</i> Genes Derived from Human Immunodeficiency Virus Type 1-Infected Patients Residing in Central Thailand. AIDS Research and Human Retroviruses, 2009, 25, 229-236.	0.5	20
79	Frequency of D222G and Q223R Hemagglutinin Mutants of Pandemic (H1N1) 2009 Influenza Virus in Japan between 2009 and 2010. PLoS ONE, 2012, 7, e30946.	1.1	20
80	An Epidemiological Analysis of Summer Influenza Epidemics in Okinawa. Internal Medicine, 2016, 55, 3579-3584.	0.3	20
81	Wing structure in the phase diagram of the Ising ferromagnet URhGe close to its tricritical point investigated by angle-resolved magnetization measurements. Physical Review B, 2017, 96, .	1.1	20
82	Highly sensitive detection of ESR1 mutations in cell-free DNA from patients with metastatic breast cancer using molecular barcode sequencing. Breast Cancer Research and Treatment, 2018, 167, 49-58.	1.1	20
83	Phenotypic studies on recombinant human immunodeficiency virus type 1 (HIV-1) containing CRF01_AE env gene derived from HIV-1-infected patient, residing in central Thailand. Microbes and Infection, 2009, 11, 334-343.	1.0	19
84	Genome-Wide Screening of Genes Required for Glycosylphosphatidylinositol Biosynthesis. PLoS ONE, 2015, 10, e0138553.	1.1	19
85	Suppression of HBV replication by the expression of nickase- and nuclease dead-Cas9. Scientific Reports, 2017, 7, 6122.	1.6	19
86	The triple helical structure and stability of collagen model peptide with 4( <i>s</i> )â€hydroxyprolylâ€proâ€gly units. Biopolymers, 2012, 98, 111-121.	1.2	18
87	Structural Basis for Dimer Formation of Human Condensin Structural Maintenance of Chromosome Proteins and Its Implications for Single-stranded DNA Recognition. Journal of Biological Chemistry, 2015, 290, 29461-29477.	1.6	18
88	Characterization of HIV-1 resistance to a fusion inhibitor, N36, derived from the gp41 amino-terminal heptad repeat. Antiviral Research, 2010, 87, 179-186.	1.9	17
89	Homo-trimeric Structure of the Type IVb Minor Pilin CofB Suggests Mechanism of CFA/III Pilus Assembly in Human Enterotoxigenic Escherichia coli. Journal of Molecular Biology, 2016, 428, 1209-1226.	2.0	17
90	The clinical and phylogenetic investigation for a nosocomial outbreak of respiratory syncytial virus infection in an adult hematoâ€oncology unit. Journal of Medical Virology, 2017, 89, 1364-1372.	2.5	17

#	Article	IF	CITATIONS
91	Apo- and Holo-structures of 3α-Hydroxysteroid Dehydrogenase fromPseudomonassp. B-0831. Journal of Biological Chemistry, 2006, 281, 31876-31884.	1.6	16
92	Generation of Rodent Malaria Parasites with a High Mutation Rate by Destructing Proofreading Activity of DNA Polymerase Î. DNA Research, 2014, 21, 439-446.	1.5	16
93	Allergic bronchopulmonary mycosis due to co-infection with Aspergillus fumigatus and Schizophyllum commune. IDCases, 2014, 1, 5-8.	0.4	16
94	Interplay of a secreted protein with type IVb pilus for efficient enterotoxigenic <i>Escherichia coli</i> colonization. Proceedings of the National Academy of Sciences of the United States of America, 2018, 115, 7422-7427.	3.3	16
95	Enterococcus saigonensis sp. nov., isolated from retail chicken meat and liver. International Journal of Systematic and Evolutionary Microbiology, 2016, 66, 3779-3785.	0.8	16
96	Complete nucleotide sequence of a plasmid containing the botulinum neurotoxin gene in Clostridium botulinum type B strain 111 isolated from an infant patient in Japan. Molecular Genetics and Genomics, 2014, 289, 1267-1274.	1.0	15
97	Field-Induced Switching of Ferro-Quadrupole Order Parameter in PrTi <sub>2</sub> Al <sub>20</sub> . Journal of the Physical Society of Japan, 2019, 88, 084707.	0.7	15
98	Emergence of infectious malignant thrombocytopenia in Japanese macaques (Macaca fuscata) by SRV-4 after transmission to a novel host. Scientific Reports, 2015, 5, 8850.	1.6	14
99	Multimodality therapy for thymoma patients with pleural dissemination. General Thoracic and Cardiovascular Surgery, 2019, 67, 524-529.	0.4	14
100	Anisotropic phase diagram of ferroquadrupolar ordering in the trigonal chiral compoundDyNi3Ga9. Physical Review B, 2019, 99, .	1.1	13
101	Genomic confirmation of nutrientâ€dependent mutability of mutators in <i>Escherichia coli</i> . Genes To Cells, 2015, 20, 972-981.	0.5	12
102	Magnetic Properties and Magnetic Phase Diagrams of Trigonal DyNi3Ga9. Journal of the Physical Society of Japan, 2017, 86, 124704.	0.7	12
103	Postnatal changes in the relative abundance of intestinal <i>Lactobacillus</i> spp. in newborn calves. Journal of Veterinary Medical Science, 2017, 79, 452-455.	0.3	12
104	Disorder-sensitive nodelike small gap in FeSe. Physical Review B, 2018, 98, .	1.1	12
105	Crystal structure of Pyrococcus horikoshii PPC protein at 1.60 Ã resolution. Proteins: Structure, Function and Bioinformatics, 2007, 67, 505-507.	1.5	11
106	Structure–activity relationship of marinostatin, a serine protease inhibitor isolated from a marine organism. Journal of Peptide Science, 2010, 16, 329-336.	0.8	11
107	Structure of the CFA/III major pilin subunit CofA from human enterotoxigenic <i>Escherichia coli</i> determined at 0.90â€Ã resolution by sulfur-SAD phasing. Acta Crystallographica Section D: Biological Crystallography, 2012, 68, 1418-1429.	2.5	11
108	Complete Genome Sequence of Ureaplasma parvum Serovar 3 Strain SV3F4, Isolated in Japan. Genome Announcements, 2014, 2, .	0.8	11

#	Article	IF	CITATIONS
109	Periodic Pattern of Genetic and Fitness Diversity during Evolution of an Artificial Cell-Like System. Molecular Biology and Evolution, 2015, 32, msv189.	3.5	11
110	Herpes zoster laryngitis in a patient treated with fingolimod. Journal of Infection and Chemotherapy, 2016, 22, 830-832.	0.8	11
111	A repeat unit of Vibrio diarrheal T3S effector subverts cytoskeletal actin homeostasis via binding to interstrand region of actin filaments. Scientific Reports, 2015, 5, 10870.	1.6	10
112	Thermodynamic Investigation of Metamagnetic Transitions and Partial Disorder in the Quasi-Kagome Kondo Lattice CePdAl. Journal of the Physical Society of Japan, 2017, 86, 034709.	0.7	10
113	Tropism of Pandemic 2009 H1N1 Influenza a Virus. Frontiers in Microbiology, 2012, 3, 128.	1.5	9
114	Functional specialization in regulation and quality control in thermal adaptive evolution. Genes To Cells, 2015, 20, 943-955.	0.5	9
115	LATS2 Positively Regulates Polycomb Repressive Complex 2. PLoS ONE, 2016, 11, e0158562.	1.1	8
116	Crystal structure of the ADP-ribosylating component of BEC, the binary enterotoxin of Clostridium perfringens. Biochemical and Biophysical Research Communications, 2016, 480, 261-267.	1.0	8
117	Field-rotational Magnetocaloric Effect: A New Experimental Technique for Accurate Measurement of the Anisotropic Magnetic Entropy. Journal of the Physical Society of Japan, 2018, 87, 073601.	0.7	8
118	Sequence-Specific and Visual Identification of the Influenza Virus NS Gene by Azobenzene-Tethered Bis-Peptide Nucleic Acid. PLoS ONE, 2013, 8, e64017.	1.1	8
119	Crystallization and preliminary X-ray analysis of the complex of NADH and 3α-hydroxysteroid dehydrogenase fromPseudomonassp. B-0831. Acta Crystallographica Section F: Structural Biology Communications, 2006, 62, 569-571.	0.7	7
120	Crystallization of human nicotinamide phosphoribosyltransferase. Acta Crystallographica Section F: Structural Biology Communications, 2007, 63, 375-377.	0.7	7
121	Stabilization Mechanism of Cytochromec552from a Moderately Thermophilic Bacterium,Hydrogenophilus thermoluteolus. Bioscience, Biotechnology and Biochemistry, 2008, 72, 2103-2109.	0.6	7
122	Reduced-Dose Telaprevir-Based Triple Antiviral Therapy for Recurrent Hepatitis C After Living Donor Liver Transplantation. Transplantation, 2014, 98, 994-999.	0.5	7
123	Magnetic Phase Transitions of the 4 <i>f</i> Skyrmion Compound EuPtSi Studied by Magnetization Measurements. Journal of the Physical Society of Japan, 2021, 90, 064701.	0.7	7
124	Crystallization and preliminary X-ray crystallographic analysis of a conserved domain in plants and prokaryotes fromPyrococcus horikoshiiOT3. Acta Crystallographica Section F: Structural Biology Communications, 2005, 61, 414-416.	0.7	6
125	Viral Detection by High-Throughput Sequencing. Methods in Molecular Biology, 2015, 1236, 125-134.	0.4	6
126	Draft Genome Sequence of <i>Plasmodium gonderi</i> , a Malaria Parasite of African Old World Monkeys. Genome Announcements, 2017, 5, .	0.8	6

#	Article	IF	CITATIONS
127	Field-Orientation Effect on Ferro-Quadrupole Order in PrTi <sub>2</sub> Al <sub>20</sub> . Journal of the Physical Society of Japan, 2020, 89, 043701.	0.7	6
128	Enantiopure Crystal Growth of a Chiral Magnet YbNi <sub>3</sub> Al <sub>9</sub> via the Flux Method with a Temperature Gradient. Journal of the Physical Society of Japan, 2020, 89, 104005.	0.7	6
129	Quasispecies of Hepatitis C Virus Participate in Cell-Specific Infectivity. Scientific Reports, 2017, 7, 45228.	1.6	5
130	Urinary tract infection due to anaerobic bacteria in a two-month-old infant. Journal of Infection and Chemotherapy, 2019, 25, 368-370.	0.8	5
131	Immunization of rabbits with synthetic peptides derived from a highly conserved β-sheet epitope region underneath the receptor binding site of influenza A virus. Biologics: Targets and Therapy, 2013, 7, 233.	3.0	4
132	Severe respiratory failure due to co-infection with human metapneumovirus and Streptococcus pneumoniae. Respiratory Medicine Case Reports, 2014, 12, 13-15.	0.2	4
133	Cloning, expression, purification, crystallization and X-ray crystallographic analysis of CofB, the minor pilin subunit of CFA/III from human enterotoxigenicEscherichia coli. Acta Crystallographica Section F, Structural Biology Communications, 2015, 71, 663-667.	0.4	4
134	WU polyomavirus detected in children with severe respiratory failure. Journal of Clinical Virology, 2018, 107, 25-28.	1.6	4
135	Diagnostic utility of metabolic parameters on FDG PET/CT for lymph node metastasis in patients with cN2 non-small cell lung cancer. BMC Cancer, 2021, 21, 983.	1.1	4
136	Peyer's Patches Play a Protective Role in Nonsteroidal Anti-inflammatory Drug-induced Enteropathy in Mice. Inflammatory Bowel Diseases, 2014, 20, 790-799.	0.9	3
137	Superconductivity and Non-Fermi-Liquid Behavior in the Heavy-Fermion Compound CeCo1â~'xNixIn5. Journal of the Physical Society of Japan, 2016, 85, 094713.	0.7	3
138	The development of large-cell carcinoma in the wall of a giant bulla complicated by hemorrhage. Surgical Case Reports, 2016, 2, 22.	0.2	3
139	Observation of a new field-induced phase transition and its concomitant quantum critical fluctuations in <mml:math xmlns:mml="http://www.w3.org/1998/Math/MathML"><mml:mtext>CeCo</mml:mtext><mml:mo>(</mml:mo> /&gt; <mml:mn>5 </mml:mn> </mml:math> . Physical Review B, 2017, 95, .	<mm1.1< td=""><td>w&gt;<sup>3</sup>mml:ms</td></mm1.1<>	w> <sup>3</sup> mml:ms
140	Anisotropic magnetic-field response of quantum critical fluctuations in Ni-doped CeCoIn5. Physical Review B, 2019, 99, .	1.1	3
141	Single Crystal Growth and Unique Electronic States of Cubic Chiral EuPtSi and Related Compounds. , 2020, , .		3
142	Thin film growth of heavy fermion chiral magnet YbNi3Al9. Applied Physics Letters, 2021, 118, 102402.	1.5	3
143	Relationship of smoking cessation period with the incidence of complications in lung cancer surgery. European Journal of Cardio-thoracic Surgery, 2022, 62, .	0.6	3
144	The role of lysine residue at amino acid position 165 of human immunodeficiency virus type 1 CRF01_AE Gag in reducing viral drug susceptibility to protease inhibitors. Virology, 2010, 405, 129-138.	1.1	2

#	Article	IF	CITATIONS
145	Cloning, expression, crystallization and preliminary X-ray crystallographic analysis of a human condensin SMC2 hinge domain with short coiled coils. Acta Crystallographica Section F: Structural Biology Communications, 2010, 66, 1067-1070.	0.7	2
146	Characterization of human immunodeficiency virus type 1 CRF01_AE env genes derived from recently infected Thai individuals. Microbes and Infection, 2014, 16, 142-152.	1.0	2
147	A case of severe soft tissue infection due to <i>Streptococcus tigurinus</i> diagnosed by necropsy in which genomic analysis was useful for clarifying its pathogenicity. Pathology International, 2018, 68, 301-306.	0.6	2
148	Low-Temperature Magnetization Measurements with Precise Two-Axis Alignment of the Sample Orientation. Journal of the Physical Society of Japan, 2018, 87, 114001.	0.7	2
149	Magnetic Ordering in Kondo Lattice Compound YbIr3Si7. Journal of the Physical Society of Japan, 2019, 88, 093705.	0.7	2
150	Diffusely Adherent <i>Escherichia coli</i> Strains Isolated from Healthy Carriers Suppress Cytokine Secretions of Epithelial Cells Stimulated by Inflammatory Substances. Infection and Immunity, 2019, 87,	1.0	2
151	Pressure Effect on the Chiral Helimagnetic Order in YbNi3Al9. Journal of the Physical Society of Japan, 2020, 89, 044715.	0.7	2
152	Magnetization and Thermal Expansion Properties of Quantum Spin Ice Candidate Pr2Zr2O7. , 2020, , .		2
153	Heavy Fermion State of YbNi2Si3 without Local Inversion Symmetry. Journal of the Physical Society of Japan, 2020, 89, 024705.	0.7	2
154	Fecal Gram staining of phagocytosed bacteria to differentiate methicillin-resistant Staphylococcus aureus: A case report. Journal of Infection and Chemotherapy, 2020, 26, 1078-1081.	0.8	2
155	Differential impacts of postoperative complications on patients' survival in completely resected non-small-cell lung cancer. General Thoracic and Cardiovascular Surgery, 2021, 69, 1283-1290.	0.4	2
156	SR-CycleGAN: super-resolution of clinical CT to micro-CT level with multi-modality super-resolution loss. Journal of Medical Imaging, 2022, 9, 024003.	0.8	2
157	Stability enhancement of cytochrome c through heme deprotonation and mutations. Biophysical Chemistry, 2009, 139, 37-41.	1.5	1
158	Pleural Invasion Depth of Disseminated Nodules in Patients with Stage IVa or Recurrent Thymoma: Assessment, Curative Impact, and Surgical Outcomes. Annals of Surgical Oncology, 2021, , 1.	0.7	1
159	Magnetization study on the ising ferromagnet URhGe with high-precision angle-resolved magnetic field near the hard axis. Progress in Nuclear Science and Technology, 2018, 5, 123-127.	0.3	1
160	Nature of field-induced antiferromagnetic order in Zn-doped <mml:math xmlns:mml="http://www.w3.org/1998/Math/MathML"&gt;<mml:msub><mml:mi>CeCoIn</mml:mi><mml:mn>5and its connection to quantum criticality in the pure compound. Physical Review B, 2022, 105, .</mml:mn></mml:msub></mml:math 	ml <b>um</b> n> </td <td>mml:msub&gt;<!--</td--></td>	mml:msub> </td
161	Cloning, expression, crystallization and preliminary X-ray characterization of cytochromec552from a moderate thermophilic bacterium,Hydrogenophilus thermoluteolus. Acta Crystallographica Section F: Structural Biology Communications, 2005, 61, 395-398.	0.7	0
162	Broad Doublet Spectra in the Quantum Paraelectric State of SrTiO3. Ferroelectrics, 2015, 485, 20-26.	0.3	0

#	Article	IF	CITATIONS
163	Soft-mode behavior in lanthanide-modified bismuth titanates. Ferroelectrics, 2017, 512, 52-57.	0.3	Ο
164	Whole-Genome Sequence of Streptococcus tigurinus Strain osk_001, Isolated from Postmortem Material. Genome Announcements, 2017, 5, .	0.8	0
165	[Regular Paper] A High-Performance Sequence Analysis Engine for Shotgun Metagenomics through GPU Acceleration. , 2018, , .		0
166	Investigation of the tricritical point of the ising ferromagnet URhGe by angle-resolved measurements. AIP Advances, 2018, 8, 101305.	0.6	0
167	Deep Learning Approach for Pathogen Detection Through Shotgun Metagenomics Sequence Classification. Lecture Notes in Computer Science, 2019, , 24-30.	1.0	0
168	Electronic Structure of Yb(Ni1â^'xCox)3Ga9 Studied by Angle-resolved Photoelectron Spectroscopy. Journal of the Physical Society of Japan, 2020, 89, 044711.	0.7	0
169	New Rare-earth Intermetallic Compounds Dy <sub>4</sub> Pd <sub>9</sub> Ga <sub>24</sub> and Er <sub>4</sub> Pd <sub>9</sub> Ga <sub>24</sub> . , 2020, , .		0
170	ASO Visual Abstract: Pleural Invasion Depth of Disseminated Nodules in Patients with StageÂlVaÂor Recurrent Thymoma: Assessment, Curative Impact, and Surgical Outcomes. Annals of Surgical Oncology, 2021, , 1.	0.7	0
171	Mucoepidermoid carcinoma of the thymus. The Journal of the Japanese Association for Chest Surgery, 2018, 32, 804-807.	0.0	0
172	Next revision of the T descriptors in the TNM classification for thymic epithelial tumors: possibilities and problems. Journal of Thoracic Disease, 2019, 11, 3217-3219.	0.6	0